Hydrogen-induced disintegration of fullerenes and nanotubes: An *ab initio* study

Savas Berber[1,2] and David Tománek[1]
[1]*Physics and Astronomy Department, Michigan State University, East Lansing, Michigan 48824-2320, USA*
[2]*Physics Department, Gebze Institute of Technology, Gebze, Kocaeli 41400, Turkey*
(Received 16 April 2009; published 24 August 2009)

We use *ab initio* density-functional calculations to study hydrogen-induced disintegration of single-wall and multiwall carbon fullerenes and nanotubes. Our results indicate that hydrogen atoms preferentially chemisorb along lines in sp^2 bonded carbon nanostructures, locally weakening the carbon bonds and releasing stress. For particular structural arrangements, hydrogen helps to relieve the accumulated stress by inducing stepwise local cleavage leading to disintegration of the outermost wall.

DOI: 10.1103/PhysRevB.80.075427 PACS number(s): 61.48.De, 64.70.Nd, 81.05.Tp, 82.65.+r

I. INTRODUCTION

Exposure to hydrogen is known to cause embrittlement in metals,[1] a major concern in materials science. It is an intriguing question, whether local decohesion due to chemisorbed hydrogen may cause similar damage in sp^2 bonded carbon nanostructures, such as fullerenes and nanotubes,[2] and whether it may have helped to efficiently cleave graphene.[3] So far, past research has focused on beneficial side effects of the interaction of hydrogen with nanocarbons, including easier separation/debundling and the prospect of reversible hydrogen storage.[2,4] Since both fullerenes and nanotubes are under internal stress due to the local curvature, hydrogen-induced local decohesion may facilitate fracture and cause irreversible damage in nanocarbons as it does in metals.[1]

Here we present an *ab initio* density-functional study of bonding and structural changes in sp^2 carbon nanostructures exposed to hydrogen. Our results indicate that hydrogen atoms preferentially chemisorb along lines on the outermost wall of single-wall and multiwall carbon fullerenes and nanotubes, locally weakening the carbon bonds and releasing stress. For particular arrangements of adsorbed hydrogen atoms, we identify the microscopic process of stepwise local cleavage leading to the disintegration of the outermost wall as a way to release the accumulated stress.

In this paper, after introducing our computational techniques, we first study the preferential adsorption sites of hydrogen on fullerenes and nanotubes. We then introduce periodically warped graphene as a useful model to investigate hydrogen-induced local bonding changes in regions of high local curvature in fullerenes and nanotubes. Next, we specify conditions, under which hydrogen-induced local stress may cause breaking of C-C bonds. We finally identify the optimum cleavage process in the stress region that leads to the eventual disintegration of the outermost wall, appearing as exfoliation of multiwall fullerenes and nanotubes.

II. COMPUTATIONAL METHODS

To gain fundamental insight into the effect of hydrogen on the structural integrity of sp^2 bonded carbon nanostructures, we studied the total energy and optimum structure of pristine and hydrogenated fullerenes and nanotubes. Our results are based on the density-functional theory within the local-density approximation and first-principles pseudopotentials. We used primarily the SIESTA (Ref. 5) code with a double-ζ basis set with polarization orbitals, the Perdew-Zunger[6] parametrization of the exchange-correlation functional, and norm-conserving *ab initio* pseudopotentials[7] in their fully separable form.[8] The accuracy of our results was verified using the PWSCF plane-wave code with ultrasoft pseudopotentials for periodic structures. We used 10^{-2} eV/Å as a strict gradient convergence criterion when determining optimum geometries. Constrained structure optimization has been used to investigate energy barriers, transition states, and generally to identify the optimum reaction pathway.

III. RESULTS

Published theoretical results include studies of the bonding character of isolated H atoms on graphite flakes, nanotubes and fullerenes,[9–11] and the preferential arrangement of hydrogen pairs on a graphene layer.[12–14] Other investigations address the relative stability of hydrogen pairs for different adsorption geometries[15] and coverages[16] of hydrogen on graphene. Theoretical studies of hydrogen-covered nanotubes focused on adsorbate-related electronic structure changes[17] and the relative stability of different adsorption arrangements.[10,15,18–20] More recent studies considered the possibility of axial cleavage in nanotubes in the presence of exohedrally adsorbed H atoms.[10,19,21] No results have been reported so far about the origin of hydrogen-induced structural damage in fullerenelike structures and its relation to stress-induced cleavage of nanotubes.

A. Local curvature in sp^2 carbon allotropes

Same as in graphene, each carbon atom in fullerenes and nanotubes has three neighbors to form very stable sp^2 bonds. Unlike in planar graphene, the most stable sp^2 carbon allotrope, stress is associated with the nonzero local curvature in fullerenes and nanotubes. The small fullerenes C_{20} and C_{60} are spherical, with all atoms equivalent and subject to the same stress. With increasing size, however, free-standing fullerenes start resembling icosahedra with 20 near-planar triangular facets spanning the surface. In these structures, stress associated with higher local curvature concentrates near the 30 edges connecting adjacent pentagons. In carbon

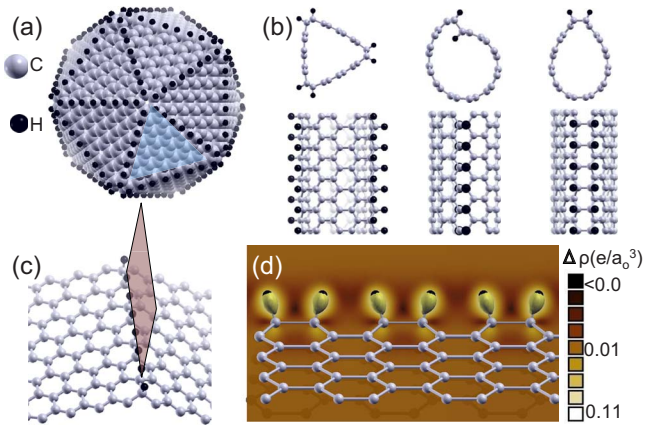

FIG. 1. (Color online) Equilibrium structure and bonding character in H-covered fullerenes and nanotubes. (a) Hydrogen chemisorption on the C_{960} fullerene along strained lines with larger curvature. (b) Lines of chemisorbed hydrogen, shown in end-on and side views, yield the most stable adsorption on the (6,6) carbon nanotube. (c) Relaxed atomic structure near a line of chemisorbed hydrogen atoms. (d) Difference charge density $\Delta\rho$ indicating hydrogen-induced $sp^2 \rightarrow sp^3$ local bonding change in graphitic nanocarbons. Contours of $\Delta\rho$ in the plane indicated in (c) are superimposed with the atomic lattice.

nanotubes, on the other hand, all atoms are equivalent and the stress associated with local curvature is distributed uniformly throughout the structure.

B. Hydrogen adsorption on single-wall and multiwall fullerenes

Even though fullerenes with more than 100 atoms have not been observed, large icosahedral shells are believed to form the outermost shell of multiwall fullerenes, called bucky onions.[22] Focusing on the faceted C_{960} hollow shell structure in Fig. 1(a), increased stress makes edge atoms more reactive and prone to bind hydrogen. Molecular hydrogen does not dissociate on planar graphene, but does so with an energy gain on fullerenes, with the dissociated hydrogen pair preferentially binding on top of adjacent carbon atoms. In the following, we will define adsorption energies per hydrogen pair, related to the free H_2 molecule. As expected, the energy gain depends on the local stress in the substrate, with values ranging from 1.20 eV at the 12 pentagonal corners to 1.35 eV at the edge sites and 0.34–0.67 eV on the facets of the C_{960} fullerene.

Calculations at higher coverages suggest that after the first two atoms are adsorbed, additional hydrogens should preferentially adsorb along straight lines on the substrate.[10] We believe that formation of this energetically preferred adsorption pattern can be achieved by surface diffusion of hydrogen atoms at temperatures found during many hydrogenation reactions since the activation barrier for sigmatropic rearrangement of chemisorbed hydrogen atoms is only ≈ 1 eV.[10] As suggested earlier and illustrated in Fig. 1(c), carbon atoms at icosahedral edges in large fullerene cages are more reactive than the facet sites. Since the dissociative chemisorption energy of hydrogen along the edges exceeds that on fullerene facets by ≈ 0.7 eV per H_2 molecule, we expect hydrogen atoms to adsorb preferentially along lines connecting pentagon corners.

C. Hydrogen adsorption on single-wall and multiwall nanotubes

Even though there are no preferential adsorption sites on a carbon nanotube, atomic hydrogen is believed to adsorb preferentially along lines parallel to the axis of the outermost tube[10,19,21] to release stress. Possible initial adsorption geometries for hydrogen on the (6,6) carbon nanotube are shown in Fig. 1(b). In the left panel, we depict the optimum nanotube geometry following hydrogen adsorption along three zigzag lines parallel to the axis. The calculated binding energy of 0.54 eV per hydrogen pair reflects also the energy associated with the tube relaxation to a triangular cross section. Presence of hydrogen apparently locally reduces the flexural rigidity of the nanotube wall, converting its circular cross section into a triangle.

Other favorable local adsorption patterns in single-wall nanotubes include exohedrally or endohedrally adsorbed hydrogens forming double lines along the nanotube axis. The initial geometry of such a combined exo/endohedral adsorption arrangement is shown in the middle panel and an exohedral double-line arrangement of hydrogens is shown in the right panel of Fig. 1(b). As we discuss later on, hydrogen-induced local decohesion causes significant structural rearrangements in both cases. The energy gain associated with hydrogen chemisorption was found to be 0.87 eV per hydrogen pair in this case.

D. Periodically warped graphene as a model strained system

To obtain fundamental insight into the origin of hydrogen-induced local decohesion that is general and independent of a particular graphitic structure, we studied the effect of a line of chemisorbed hydrogen atoms on the structure and bonding in a graphene layer, as shown in Fig. 1(c). Hydrogen atoms bind preferentially on top of carbon atoms, causing a local buckling. A line of chemisorbed hydrogen atoms is expected to form a crease in the initially planar graphene.[3] With the imposed boundary conditions, this structural change is represented by periodically warping the graphene layer. In Fig. 1(c) we constrained the crease angle to equal that between adjacent facets on the icosahedron in Fig. 1(a). To get insight into the nature of the adsorption bond, we inspected the charge-density difference $\Delta\rho = \rho(\mathrm{H/graphene}) - \rho(\mathrm{H}) - \rho(\mathrm{graphene})$, representing the charge redistribution in the system upon hydrogen adsorption. The spatial distribution of $\Delta\rho(\mathbf{r})$ is shown in Fig. 1(d) in the plane schematically indicated in Fig. 1(c). Hydrogen adsorption causes only local charge rearrangement leading to a charge accumulation in the H-C σ bonds, depleting the charge in the local C-C bond region, as expected in case of sp^3 bonding. Both the charge rearrangement and the local buckling are strong indicators for a local $sp^2 \rightarrow sp^3$ transition. As suggested above, hydrogen pairs bind preferentially to neighboring carbon atoms, thereby changing an initially strong sp^2 bond to a weaker, strained sp^3 bond. This local decohesion resembles to some

degree the microscopic mechanism of hydrogen embrittlement in some metals.[1]

E. Hydrogen-induced stress regions in single-wall and multiwall fullerenes

Besides decohesion, local change from sp^2 to sp^3 bonding is also associated with a net increase in the C-C bond length by typically 8%. In partially hydrogen-covered systems, carbon atoms connected to lines of hydrogen are under stress. The consequences can be best illustrated in the fullerene structure shown in Fig. 1(a), where hydrogen only attaches to the edges. The hydrogen-free planar facets can be thought as incompressible, same as small graphene flakes. Since the corners of the triangular facets determine the edge length, sp^3 bonded carbon atoms along the edges are prevented from increasing their interatomic distance, subjecting the edges to stress. The energy associated with accumulated stress increases linearly with the edge length L. For a critical value L_{crit}, this energy will exceed the activation barrier ΔE to break a C-C bond as a first step to initiating a cleavage that eventually causes the disintegration of the structure.

As we show later on, we find that $\Delta E \approx 1.7$ eV. This amount of stress energy is accumulated in a hydrogenated fullerene edge of critical length $L_{crit} \approx 15$ nm. We thus expect hydrogen-induced cleavage to occur only in fullerenes with $L > 15$ nm, with a diameter exceeding ≈ 28 nm and containing more than 10^5 C atoms. Such large fullerenes never occur as single-wall structures but may form the outermost wall of a multiwall bucky onion. In large bucky onions, the spherical walls inside exert radial pressure on the outermost wall, thus enhancing the hydrogen-induced stress and reducing the critical diameter for disintegration of the outermost wall. We expect that multiwall fullerenes exposed to hydrogen should peel layer by layer from the outside in a process appearing as exfoliation.

F. Mechanism of hydrogen-induced cleavage in periodically warped graphene

In the following, we study the microscopic mechanism leading to cleavage at the minimum-energy cost. To obtain a general understanding of the fracture process that does not depend on a particular system, we created generic creases by placing a periodic array of hydrogen lines along the armchair direction on alternating sides of an infinite graphene monolayer, as seen in Fig. 2(a). The energetics and atomic arrangement during the initial cleavage are depicted in Figs. 2(b) and 2(c). Cleavage at the crease is caused by locally weakening the affected bonds. We found that this is best achieved by adsorbing additional hydrogen atom pairs on both sides of the initial hydrogen line, as shown in the left panel of Fig. 2(c). Such a local arrangement of adsorbed hydrogens is a favorable prerequisite to cleave an edge segment. We found that the energy needed to break one bond is larger than the energy to break two adjacent bonds, shown in a dark color in the left panel of Fig. 2(c). Continuing this concerted bond breaking mechanism should cleave the edge, causing the structure to disintegrate.

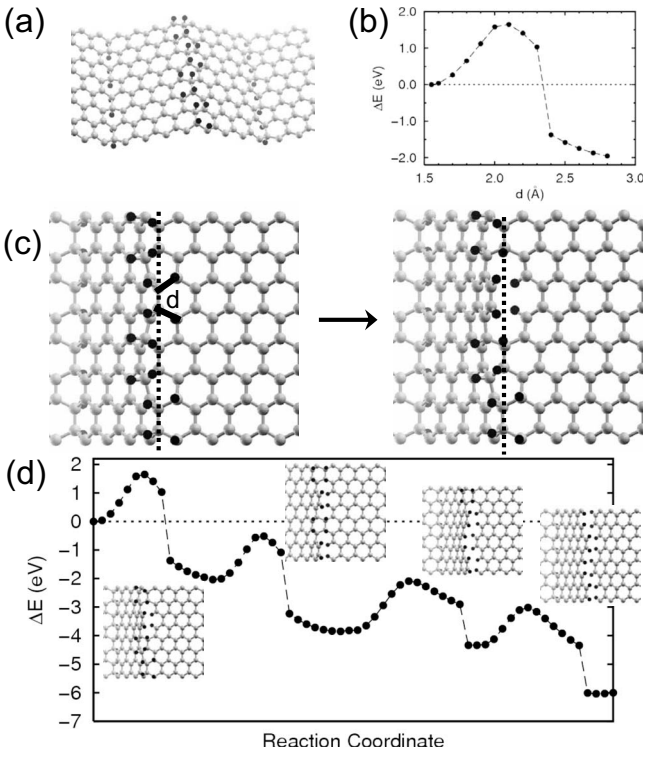

FIG. 2. Zipper mechanism of hydrogen-induced disintegration of strained sp^2 carbon nanostructures. (a) Periodically warped graphene as model strained system. (b) Optimum structure and energetics for breaking a bond pair. (c) Sequence of bond cleavages resulting in a crack.

The energetics of cleavage in Fig. 2(b) shows the total-energy change with respect to the initial structure as a function of the bond length d across the crack, which we use as the reaction coordinate. We consider the full range of d values occurring during the cleavage reaction and, for each value of d, we globally optimize the structure. Consequently, the calculated transition paths for the disintegration of hydrogenated fullerenes and nanotubes represent the optimum cleavage path in unconstrained systems. Following an initial energy investment of 1.7 eV, the bonds break abruptly, leading to the final structure depicted in the right panel of Fig. 2(c). There is a net energy gain of ≈ 2 eV associated with the bond breaking, caused by releasing the accumulated stress. The initially stressed sp^3 bonded crease segment converts into a pair of more stable sp^2 bonded, hydrogen-terminated graphene edges.

We next calculated the energy barriers associated with breaking specific bonds in search of the optimum pathway to complete the crease cleavage after it was initiated. The optimum sequence of bonds to break, along with the intermediate structures and the energetics of the process, is depicted in Fig. 2(d). Interestingly, the smallest energy investment to propagate the fracture following the first step in Fig. 2(b) does not involve the neighboring pair of C-C bonds on the opposite side of the ridge but rather the more distant pair of C-C bonds on the same side of the ridge. Our results indicate that the energy barrier to propagate the fracture decreases at successive steps. As a matter of fact, it may be reasonable to assume that the energy released following the initial step

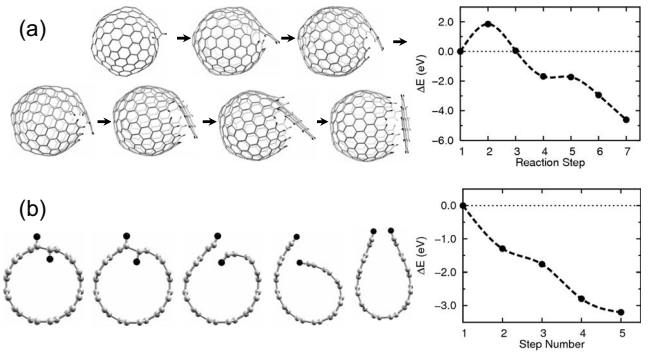

FIG. 3. Hydrogen-assisted disintegration of (a) the C_{240} fullerene and (b) the (6,6) carbon nanotube. Structural snapshots along the optimum reaction pathway are depicted in the left panels. The structural transformations of the nanotube in (b) are shown in end-on view. Carbon atoms are shown as gray and hydrogen atoms as larger black spheres. The right panels show the total-energy change in the system with the data points corresponding to the structures in the left panels.

may activate the zipperlike cleavage at the crease without further energy investment. Once cleavage is initiated, the unzipping process transforms the stressed crease into two overlapping graphene edges in an exothermic reaction.

G. Optimum pathway of the hydrogen-induced disintegration of fullerenes: From C_{240} to multiwall structures

Having studied the microscopic cleavage process in the warped graphene model, we next turn to hydrogen-induced disintegration of specific fullerene and nanotube structures. As we discussed above, we expect hydrogen-induced disintegration to proceed spontaneously only in very large fullerenes, which are typically multiwall structures. Even the disintegration pathway does not depend on the size, we find this reaction to be energetically activated in the smaller C_{240} fullerene. The energetics of the C_{240} disintegration process, induced by hydrogen adsorption along the icosahedral edges, is shown in Fig. 3(a) along with snapshots of intermediate structures. Unlike in the model system addressed in Fig. 2, the hydrogen coverage has been gradually increased as the cleavage progressed, as an alternative scenario to initiating unzipping. Both in the warped graphene model and in the C_{240} fullerene, we find the disintegration process to be exothermic, following an initial energy investment of ≈ 2 eV.

H. Optimum pathway of the hydrogen-induced disintegration of single-wall and multiwall nanotubes

Whereas large fullerenes are more susceptible to hydrogen-induced fracture due to the stress buildup in the hydrogenated edges, we find nanotubes that are narrow to be more susceptible to fracture due to the stress caused by their high uniform curvature. Both in fullerenes and nanotubes with multiple walls, hydrogen will first adsorb on the outermost wall, causing local decohesion leading to bond breaking and eventual disintegration of the outermost wall. Continuing exposure to hydrogen will cause a layer-by-layer peeling that will appear as exfoliation.

As suggested by our results in Fig. 1(b), hydrogen adsorption concentrates the deformation along lines parallel to the tube axis, reducing the flexural stress in the hydrogen-free region. The right panels of Fig. 1(b), depicting hydrogen-covered nanotubes, illustrate how hydrogen-induced decohesion along adsorption lines may cause large structural changes. The detailed cleavage process of a (6,6) carbon nanotube, covered by a complete chain of hydrogens adsorbed exohedrally and by an adjacent chain adsorbed endohedrally, is depicted in Fig. 3(b). Our numerical results for an infinite nanotube are obtained using periodic boundary conditions and the primitive axial unit cell. The sequence of snapshots, presented in an end-on view, depicts intermediate structures, including a scroll,[23] encountered during a conjugate gradient optimization from an unrelaxed initial structure. This process is only spontaneous if all hydrogens adsorb in the optimum way to form completely filled lines of adsorbed hydrogen and is activated otherwise. The final structure with a horseshoelike cross section, stabilized by the attraction of the hydrogenated zigzag edges, may furthermore undergo an activated conversion to a planar graphene strip with hydrogen-terminated edges.

IV. SUMMARY AND CONCLUSIONS

In conclusion, we used *ab initio* density-functional calculations to study hydrogen-induced disintegration of single-wall and multiwall carbon fullerenes and nanotubes. Our results indicate that hydrogen atoms preferentially chemisorb along lines in sp^2 bonded carbon nanostructures, locally weakening the carbon bonds and releasing stress. Contrary to common belief that chemisorbed hydrogen causes no harm to carbon nanostructures, we show that irreversible structural changes may be caused by chemisorbed hydrogen that can initiate local cleavage leading to the disintegration of the outermost wall. In experimental observations of multiwall structures, this could be interpreted as hydrogen-induced exfoliation.

ACKNOWLEDGMENTS

We thank Glen P. Miller for inspiring this study by his experimental observations in bucky onions. This work was funded by the National Science Foundation under NSF-NSEC Grant No. 425826 and NSF-NIRT Grant No. ECS-0506309. Computational resources have been provided by the Michigan State University High Performance Computing Center.

[1] W. Zhong, Y. Cai, and D. Tomanek, Nature (London) **362**, 435 (1993).
[2] M. Dresselhaus, G. Dresselhaus, and P. Eklund, *Science of Fullerenes and Carbon Nanotubes* (Academic, San Diego, 1996).
[3] X. Li, X. Wang, L. Zhang, S. Lee, and H. Dai, Science **319**, 1229 (2008).
[4] A. Jorio, M. Dresselhaus, and G. E. Dresselhaus, *Carbon Nanotubes: Advanced Topics in the Synthesis, Structure, Properties and Applications*, Topics in Applied Physics Vol. 111 (Springer, New York, 2008).
[5] J. M. Soler, E. Artacho, J. D. Gale, A. García, J. Junquera, P. Ordejón, and D. Sánchez-Portal, J. Phys.: Condens. Matter **14**, 2745 (2002).
[6] J. P. Perdew and A. Zunger, Phys. Rev. B **23**, 5048 (1981).
[7] N. Troullier and J. L. Martins, Phys. Rev. B **43**, 1993 (1991).
[8] L. Kleinman and D. M. Bylander, Phys. Rev. Lett. **48**, 1425 (1982).
[9] L. Jeloaica and V. Sidis, Chem. Phys. Lett. **300**, 157 (1999).
[10] G. Miller, J. Kintigh, E. Kim, P. Weck, S. Berber, and D. Tomanek, J. Am. Chem. Soc. **130**, 2296 (2008).
[11] E. Kim, P. F. Weck, S. Berber, and D. Tomanek, Phys. Rev. B **78**, 113404 (2008).
[12] A. Allouche, A. Jelea, F. Marinelli, and Y. Ferro, Phys. Scr. **T124**, 91 (2006).
[13] T. Roman, W. A. Diño, H. Nakanishi, H. Kasai, T. Sugimoto, and K. Tange, Carbon **45**, 218 (2007).
[14] L. Hornekaer, E. Rauls, W. Xu, Z. Šljivančanin, R. Otero, I. Stensgaard, E. Laegsgaard, B. Hammer, and F. Besenbacher, Phys. Rev. Lett. **97**, 186102 (2006).
[15] D. Stojkovic, P. Zhang, P. E. Lammert, and V. H. Crespi, Phys. Rev. B **68**, 195406 (2003).
[16] A. Allouche and Y. Ferro, Phys. Rev. B **74**, 235426 (2006).
[17] O. Gülseren, T. Yildirim, and S. Ciraci, Phys. Rev. B **66**, 121401(R) (2002).
[18] T. Yildirim, O. Gülseren, and S. Ciraci, Phys. Rev. B **64**, 075404 (2001).
[19] J. S. Arellano, L. M. Molina, A. Rubio, M. J. López, and J. A. Alonso, J. Chem. Phys. **117**, 2281 (2002).
[20] O. Gülseren, T. Yildirim, and S. Ciraci, Phys. Rev. B **68**, 115419 (2003).
[21] G. Lu, H. Scudder, and N. Kioussis, Phys. Rev. B **68**, 205416 (2003).
[22] D. Ugarte, Nature (London) **359**, 707 (1992).
[23] J. G. Lavin, S. Subramoney, R. S. Ruoff, S. Berber, and D. Tomanek, Carbon **40**, 1123 (2002).